Surface & Coatings Technology 521 (2026) 133104

Contents lists available at ScienceDirect

Surface & Coatings Technology

journal homepage: www.elsevier.com/locate/sct

Full length article

Continuous superposition of high power pulses and radio frequency power on a single magnetron target

J. Müller [a,*], J. Swoboda [a], F. Burmeister [a], A. Fromm [a], M. Wirth [a], A. Killinger [b], S. Ulrich [c]

[a] Fraunhofer Institute for Mechanics of Materials (IWM), Wöhlerstr. 11, Freiburg 79108, Germany
[b] Institute for Manufacturing Technologies of Ceramic Components and Composites (IFKB), University of Stuttgart, Stuttgart 70569, Germany
[c] Institute for Applied Materials (IAM-AWP), Karlsruhe Institute of Technology (KIT), Karlsruhe 76021, Germany

ARTICLE INFO

Keywords:
HiPIMS
RF
Superposition
Hybrid

ABSTRACT

High Power Impulse Magnetron Sputtering (HiPIMS) offers significant advantages over established sputtering techniques such as DC, MF, or RF sputtering. Thin films deposited with HiPIMS exhibit improved properties but often suffer from low deposition rates. In addition, reactive HiPIMS processes tend to arc. Superposition of different plasma excitations may help to overcome these limitations. We investigated the superposition of HiPIMS and RF on a single magnetron and studied voltage–current characteristics as well as the influence of pressure on process stability and cathode voltage for the reactive and non-reactive deposition of Aluminium in Ar/O2 discharge. We found that superimposing RF onto HiPIMS allows for stable operation at lower pressures and reduces arcing. Notably, the effect of the superimposed RF on peak current differs by mode: in reactive sputtering, the HiPIMS peak current is increased, while in non-reactive mode, the peak current is decreased. This is attributed to the different secondary electron emission in non-reactive and reactive mode.

1. Introduction

Magnetron sputtering is a widely used and well-established technique for depositing thin films for various applications [1]. High Power Impulse Magnetron Sputtering (HiPIMS) is a variant that offers significant advantages over established techniques such as DC, MF, and RF sputtering. The extremely high peak currents and voltages during a HiPIMS pulse, lead to high plasma densities and contribute to a higher kinetic energy as well as to a higher degree of ionization of the sputtered species [2–8].

Thin films deposited with HiPIMS exhibit improved properties such as high density [9], smooth film surface, increased film adhesion, resistance to wear, corrosion and oxidation [7,10–13] and enhanced conformal coverage of non-planar substrates [2,7,14]. However, due to a low duty cycle and self-sputtering effects [15], HiPIMS features low deposition rates compared to conventional PVD methods for non-reactive and many reactive deposition processes [9,16–20]. In general, reactive sputtering is used for the deposition of compound materials from a metallic target by adding reactive gases to the deposition chamber. However, metallic targets tend to poison in a reactive deposition process and therefore develop a dielectric film on the surface, which can change the plasma potential and result in arcing, which in turn, leads to the ejection of macro-particles from the target [21,22], creating distinct coating defects [23]. Reactive HiPIMS may even switch to cathodic arc discharge [24]. Early works on HiPIMS sputtering of compound films in a HiPIMS process, used an arc suppression system [25] that detects arcs electrically and disconnects the power supply for a short period of time. However, this approach does not address the root cause of the instability of the HiPIMS process. Tiron et al. 2020 [26] demonstrated, that arcing can be significantly reduced by applying ultra-short pulses (below 5 μs) to the target. Another approach consists of superposition of HiPIMS with a second kind of plasma excitation which is not prone to arcing, e.g. bipolar DC-, MF- or RF-Sputtering which is a frequently employed technology for the deposition of compounds, due to the effective suppression of charge build-up on the target's surface. Superposition of different plasma excitations has been realized by sputtering from multiple targets where at least one target is operated in HiPIMS mode (Co-Sputtering). Hybrid HiPIMS/RF-Systems have already been established in co-sputtering setups [27,28] where one cathode is powered by a HiPIMS generator and another cathode by a RF power supply. Other works succeeded to incorporate the advantages of HiPIMS into hybrid deposition systems, superimposing additional DC [29–31] and MF [19,32–36].

We present what is, to the best of our knowledge, the first study of the electrical effects of a continuous superposition of a high power pulses and RF power on a single magnetron target. Specifically, we

* Corresponding author.
E-mail address: jonas.mueller@iwm.fraunhofer.de (J. Müller).

https://doi.org/10.1016/j.surfcoat.2025.133104
Received 10 October 2025; Received in revised form 6 December 2025; Accepted 21 December 2025
Available online 22 December 2025

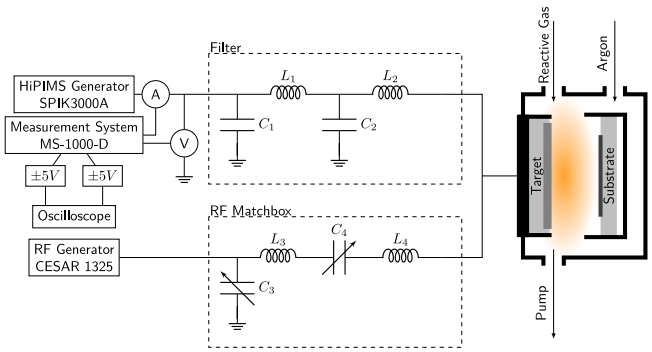

Fig. 1. Wiring schematic of the HiPIMS/RF circuit, used in the experiments. The low-pass-filter protects the HiPIMS generator from the RF signal. Voltage and current of the individual HiPIMS pulses are measured between the HiPIMS-generator and the RF filter, using a Melec measurement system (MS-1000-D) and an oscilloscope.

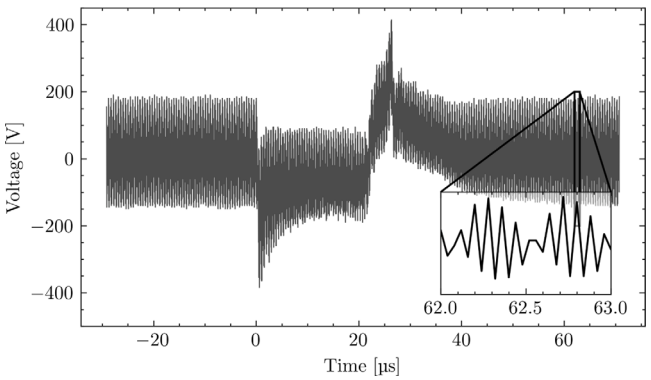

Fig. 2. Voltage measurement of continuously superimposed HiPIMS/RF measured directly at the sputter source. The HiPIMS pulse appears "noisy" due to the superimposed RF oscillation. 13.56 MHz corresponds to 13.56 wave cycles within 1 µs. Voltage variation with frequencies lower than 13,56 MHz visible in the inset are probably due to instrumental issues and sampling rates. The HiPIMS pulse on-time was set to 20 µs.

investigate how the target voltage and peak current of the HiPIMS pulse are affected by the addition of continuous RF power, and whether pre-ionization from the sustained RF plasma can enhance the HiPIMS peak current.

2. Method

We modified a sputter coater from FHR (Ottendorf, Germany) with a CESAR 1325 RF Generator from Advanced Energy, a SPIK3000A-EF-05 pulsing unit from Melec GmbH (Baden–Baden, Germany) and connected both to the same magnetron assembly [37,38]. An industrial-sized metallic Aluminium target with purity of 3N a size of 400 × 90 × 8 mm (360 cm^2) was used in the experiments. The HiPIMS generator is specified for a maximum pulse output voltage of 1000 V and pulsed peak power of 500 kW. The electric wiring is shown schematically in Fig. 1. A custom-built low-pass filter by Aurion Anlagentechnik GmbH (Seligenstadt, Germany) was installed between the HiPIMS generator and the target in order to protect the generator from potential damage due to backreflections of the RF power. This configuration was utilized in a similar manner in earlier works, in which RF was superimposed on DC [39–41] and pulsed DC [42], but not on HiPIMS.

The vacuum chamber was evacuated to a base pressure of $8 * 10^{-6}$ Pa. HiPIMS and RF have been superimposed continuously. The pressure during deposition was varied from 0.02 to 1.4 Pa with a vacuum control valve from VAT, using pressure control mode.

The resulting voltages and currents for the HiPIMS-pulse were recorded using a Melec measurement system MS-1000-D and a digital oscilloscope. The measurement probes are placed between the Low-Pass-Filter and the HiPIMS generator. Therefore, the measurements show the filtered HiPIMS pulses without superimposed RF. However, the effect of the superimposed RF is directly recognizable in the offset of the HiPIMS voltage due to the RF self bias (see e.g. Fig. 6). The HiPIMS pulse on- and off-times, are adjusted for each experiment in order to achieve stable plasma conditions, the values are given in the figure subscripts.

For illustrative purposes, the voltage of the continuous superposition of HiPIMS and RF was uniquely measured directly at the magnetron assembly with a custom-build RF-sensing head. The result is shown in Fig. 2, where the HiPIMS pulse is clearly visible. The apparent 'signal noise' is due to the 13.56 MHz RF voltage.

3. Results

3.1. I-U-characteristics

Current–voltage characteristics (I–U) were measured in voltage control mode to isolate the intrinsic plasma response from generator control algorithms. For each data point, the voltage was set manually and held constant while the resulting discharge current was recorded after reaching steady state (typically 30–60 s). For the non-reactive (see Fig. 3) and reactive mode (Fig. 4) the pressure was kept constant at 1 Pa. The voltage was incrementally increased up to the generator's maximum output of 1 kV. The plotted peak current density represents the nominal current density, calculated as the peak current divided by the total target area (360 cm^2). Using the racetrack area for the calculation of the current density would provide a more physically meaningful measure, but is difficult to determine accurately, as it varies with pressure and the total applied current [24].

The conventional DC magnetron I-U characteristics follow a power law $I = kU^n$ with n up to 18 [43]. For HiPIMS, the exponent n reaches low values down to 1 [3,43], indicating the transition to a pure HiPIMS-regime with high flux densities. In this work, the exponent n was determined by a linear regression fit of the I-U data at the lower and upper end of the applied voltage range, as shown in Figs. 3 and 4.

3.1.1. Non-reactive deposition of aluminium

The I-U-characteristics of the non-reactive mode is shown in Fig. 3 where the HiPIMS pulse length was set to 40 µs. As expected from earlier works (e.g. Magnus et al. 2011 [44]), the peak current increases with increasing voltage. In pure HiPIMS mode, the peak current increases in the range from 11 A at 460 V, up to 490 A at 1 kV. This corresponds to a peak current density from 32 mA cm^{-2} to 1361 mA cm^{-2}, resulting in the exponent n to start at roughly $n = 11$ between 400 V and 500 V and approximately $n = 2.1$ for voltage between 900–1000 V. A qualitatively similar behaviour has been observed by Alami et al. [43] and Ehiasarian et al. [3] and will be discussed below. A 500 mA cm^{-2} threshold is marked by the blue dashed line in the I–U plots for better visualization. While this threshold is commonly referenced in the literature as indicative of HiPIMS operation [45], it should be noted that, in the absence of plasma ionization measurement, it is meant as a visual guide only.

When adding 500 W of RF-power to the non-reactive HiPIMS process, we have observed, that this results in lower peak currents, when compared to pure HiPIMS. Especially at low HiPIMS voltages, the peak current is significantly decreased and only starts to increase at voltages above approximately 700 V. The peak current density varies in the range of 20 mA cm^{-2} up to 1145 mA cm^{-2} at 1 kV, not reaching the maximum peak current of the pure HiPIMS process. The value of the power law exponent is approximately $n = 1$ for low target voltages, significantly increases between 650 and 750 V and again decreases to $n = 2.4$ at high voltages between 900 V and 1 kV.

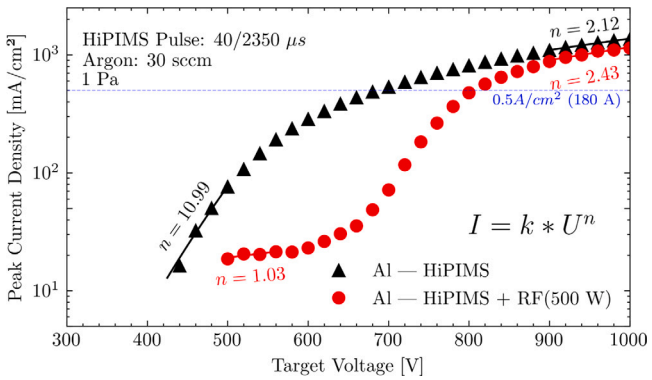

Fig. 3. I-U-characteristics for non-reactive deposition mode. The exponent n is calculated by linear regression, assuming a power law $I = kU^n$. The peak current density in pure HiPIMS is higher when compared to hybrid HiPIMS/RF mode. Peak current density threshold of 0.5 A cm^{-2} plotted for reference.

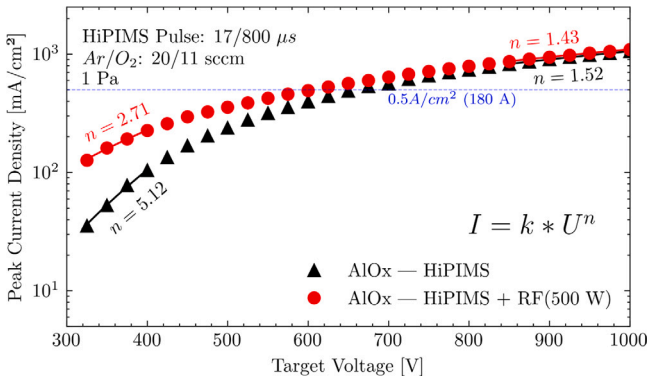

Fig. 4. I–U-characteristics for reactive deposition mode. Contrary to the non-reactive mode, the peak current densities are generally lower in pure HiPIMS, compared to hybrid HiPIMS/RF. 0.5 A cm^{-2} threshold plotted for reference.

3.1.2. Reactive deposition of aluminiumoxide

For reactive deposition of Aluminiumoxide, we introduced 11 sccm O_2 and 20 sccm Ar in the deposition chamber to keep the total gas flow approximately constant. Based on preliminary recordings of hysteresis curves (not shown), this corresponds to operation in poisoned mode. The HiPIMS pulse on-time was reduced to 17 μs for the reactive process to ensure stable operation and to minimize arcing. For many reactive HiPIMS processes, one would expect higher peak currents than in non-reactive mode, due to higher secondary electron emission yield for many oxides and especially Aluminiumoxide compared to pure metals [44,46–48]. However, in this case, the recorded peak currents are in the same range as in non-reactive mode, but this is simply attributed to the shorter on-time of the HiPIMS pulse. In pure HiPIMS mode, the peak current increases in the range of 35 mA cm^{-2} at 325 V to 1050 mA cm^{-2} at 1 kV.

Contrary to the non-reactive deposition before, in reactive mode, the peak current is increased when 500 W of RF is added to the process, especially at lower HiPIMS voltages. At 325 V, the reactive HiPIMS process inexhibits a peak current density of 35 mA cm^{-2}, while the superimposed HiPIMS+RF process exhibits 125 mA cm^{-2}. With increasing HiPIMS voltage, the peak currents of both processes start to converge until the maximum peak current of 1050 mA cm^{-2} (HiPIMS), respectively 1100 mA cm^{-2} (HiPIMS+RF) is reached at 1 kV.

3.2. Effects of pressure variation

One important process parameter in PVD processes is the chamber pressure, which is correlated to the mean free path of gas species in the plasma and is related to the ionization probability of working gas atoms. We investigated which pressure regimes are accessible in HiPIMS and superimposed HiPIMS+RF, expecting lower possible pressure in superimposed mode due to preionization, as reported by Holtzer et al. [27] for HiPIMS and RF co-sputtering from two magnetron targets. For the pressure variations, HiPIMS power was fixed at 1 kW in power-control mode, contrary to the conditions for the recording of the I-U curves (voltage control mode).

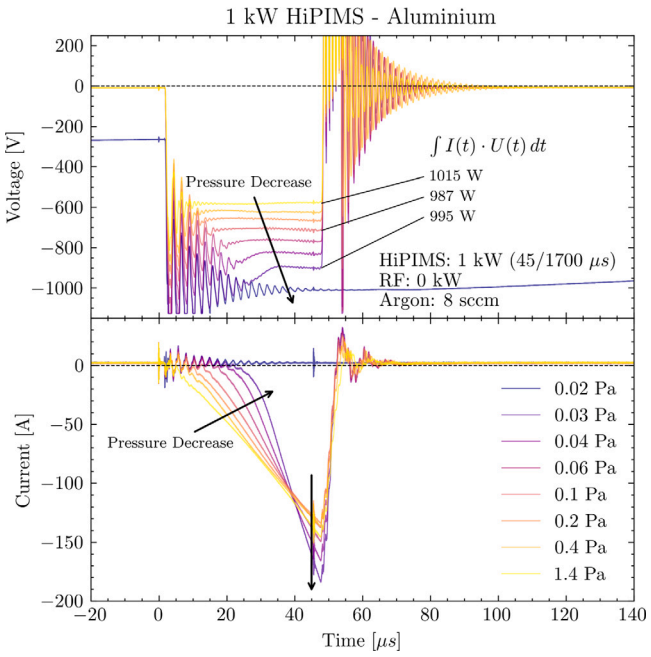

Fig. 5. Voltage and current during HiPIMS pulse measured for non-reactive HiPIMS deposition of Aluminium. Black arrows indicate direction of pressure decrease. The voltage and peak current increases with decreasing pressure, while the current onset is delayed with decreasing chamber pressure. At 0.02 Pa the pressure was too low to successfully sustain a plasma.

The average power was also calculated by integrating the product of the time-dependent currents and voltages ($\int I(t) \cdot U(t)\, dt$). The resulting values matched the power readings provided by the HiPIMS generator software and are depicted in Figs. 5–8.

3.2.1. Pressure variation in non-reactive HiPIMS

For the non-reactive case, Ar flow rate was set to 8 sccm. The pressure was decreased from 1.4 Pa to 0.02 Pa. The resulting temporal evolution of voltage and current is shown in Fig. 5. We observed that the target voltage increases from 575 V to 900 V with decreasing chamber pressure. This is a direct consequence of the chosen power control mode. Reduced pressure means less gas particles, therefore less potential charge carriers and results in generally lower current. The time needed to establish a stable voltage is prolonged with decreased pressure. This is also reflected in the current onset, which starts later at lower pressure. At p = 0.03 Pa, the real pulse duration is approximately one third of the total set pulse time, due to the delay in current onset of approximately 25 μs. In order to keep the average power of 1 kW constant, the software increases the generator voltage to keep the time-averaged product $U * I$ constant. Paradoxically, this combination of increased voltage and later current onset results in increasing peak current with decreasing pressure. At 0.02 Pa the pressure was too low to successfully sustain a plasma, the power supply ran into its voltage limit of 1000 V, while the discharge current dropped to zero ampere. Similar behaviour was also observed at higher HiPIMS power of 1.5 kW but not further investigated in this work.

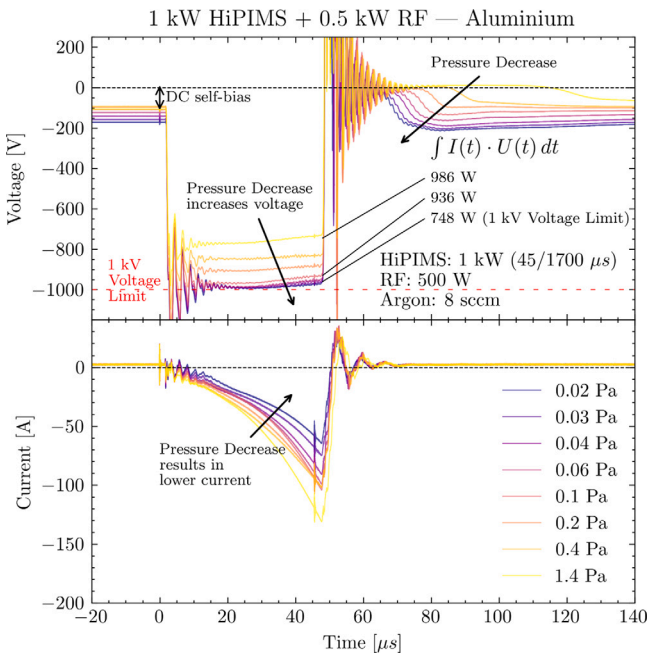

Fig. 6. Voltage and current of HiPIMS pulse measured for non-reactive deposition of Aluminium in superimposed HiPIMS/RF mode.

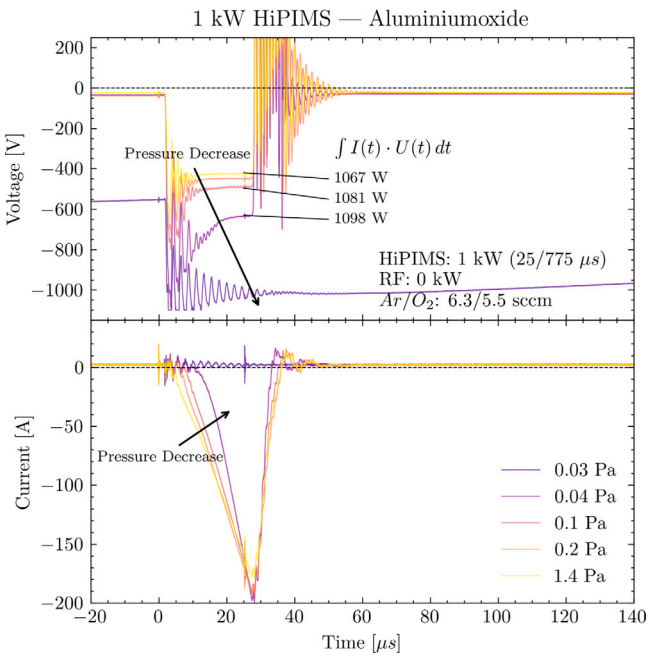

Fig. 7. Voltage and current of HiPIMS pulse for reactive deposition of Aluminiumoxide in pure HiPIMS mode. The voltage increases with decreasing pressure, while the current onset is delayed with decreasing chamber pressure. At 0.03 Pa the pressure was too low to successfully sustain a plasma.

When superimposing 500 W of RF power to the non-reactive HiPIMS process, the HiPIMS current is generally decreased (see Fig. 6). This is expected from the I-U characteristics, as shown before. The current starts to increase earlier in superimposed mode. This behaviour is attributed to the faster stabilization of the HiPIMS voltage, especially at lower pressure. This is counteracted by the generator's control software which again increases the voltage in order to maintain the set average power of 1 kW as explained before. The combination of this competing effects results in generally lower peak current density of the superimposed mode, while maintaining 1 kW of constant HiPIMS power (see calculated average power, based on the product of the time-dependent currents and voltages).

The superimposed RF induces a DC self-bias, not blocked by the low-pass filter, and therefore visible in the time–voltage plots in Fig. 6 as explained in the experimental section. The temporal suppression of the DC self-bias during the pulse is attributed to a breakdown of the dark space above the target's surface and the accompanying potential drop. After the HiPIMS pulse, the DC self-bias is restored within 10–60 μs. The recovery time decreases with lower pressure. Compared to pure HiPIMS, the HiPIMS+RF process can be operated at lower chamber pressures, down to 0.02 Pa.

With decreasing pressure, the peak current is generally decreased. This observation is in line with the I-U characteristics, investigated before and also counteracted by the generator's control software by increasing the voltage in order to maintain 1 kW of average power. As a result, the voltages in superimposed mode are generally higher when compared to pure HiPIMS.

However, especially at pressures below 0.1 Pa, the set power of 1 kW could not be reached due to the generator's voltage limits of 1 kV.

3.2.2. *Pressure variation in reactive HiPIMS*

The same measurements were conducted for reactive deposition of Aluminiumoxide. The reactive gas flow was set to 6.3 sccm Ar and 5.5 sccm O_2. According to preliminary sputter hysteresis experiments (not shown), this corresponded to sputtering in poisoned mode. To achieve stable plasma conditions, the HiPIMS pulse on-time was reduced from 45 to 25 μs, while the frequency was increased by reducing the off-time from 1700 to 775 μs in order to achieve approximately comparable peak currents in the range of 150–200 A at 1 kW of average power in HiPIMS mode.

As observed before in non-reactive deposition, the voltage increases with decreasing pressure (see Fig. 7), to compensate for reduced current at lower pressure and maintain the constant averaged power of 1 kW.

When the additional 500 W RF power is superimposed to the reactive HiPIMS process, the voltage of the HiPIMS generator decreases. This behaviour is assigned to the generator's control software attempt to maintain 1 kW of power and is in line with the earlier investigated reactive I-U characteristic (Fig. 8), where it was observed, that a superimposed RF power results in higher currents.

The application of superimposed RF power results in a DC self-bias (see Fig. 8), consistent with observations in the non-reactive mode. However, the DC self-bias takes noticeably longer to recover at lower deposition pressures, which contrasts with the faster recovery observed under equivalent conditions in non-reactive processes.

The voltage is generally lower than in non-reactive deposition mode, while the peak currents are generally higher and not as much affected by changes in pressure as in non-reactive deposition. This is an expected behaviour due to higher secondary electron emission in reactive mode as described by Magnus et al. 2011 [44]. The onset of current is delayed with decreasing pressure. The peak currents in the reactive HiPIMS+RF-mode are lower, when compared to the pure HiPIMS. This behaviour might appear counter-intuitive at first sight (especially when compared with reactive I-U characteristics) but is attributed to the earlier stabilization of voltage in HiPIMS+RF mode, resulting in an earlier increase of the current and therefore increased current-time integral (average power) in the chosen power control mode.

Fig. 9 summarizes the aggregated peak currents from Figs. 5–8 for the four operational modes (note that in Figs. 5–8 not all recorded I-U-curves are plotted for the sake of clarity). Both, non-reactive and reactive HiPIMS+RF process can be operated at lower pressures, when compared to pure HiPIMS.

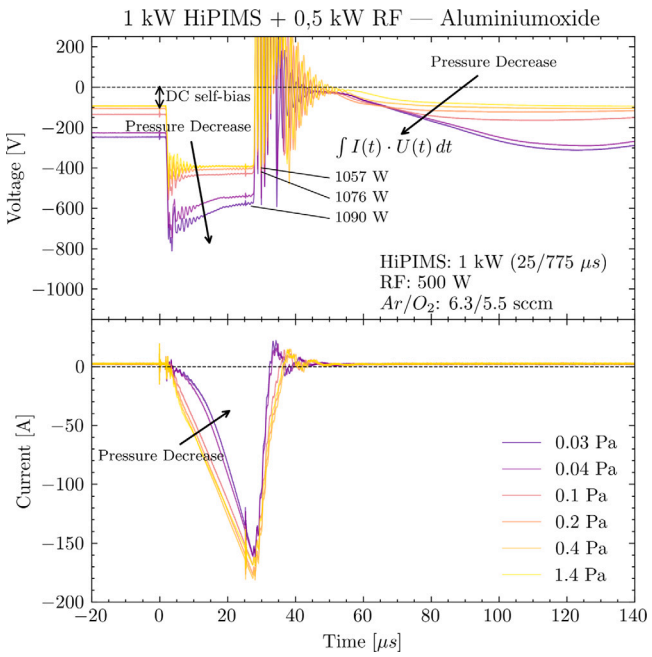

Fig. 8. Voltage and current of HiPIMS pulse for reactive deposition of Aluminiumoxide in superimposed HiPIMS/RF mode. Compared to pure HiPIMS mode, the peak current decreases with decreasing chamber pressure, which is contrary to the behaviour in pure HiPIMS mode. For superimposed HiPIMS/RF mode, a stable process can be established at lower pressures than in pure HiPIMS.

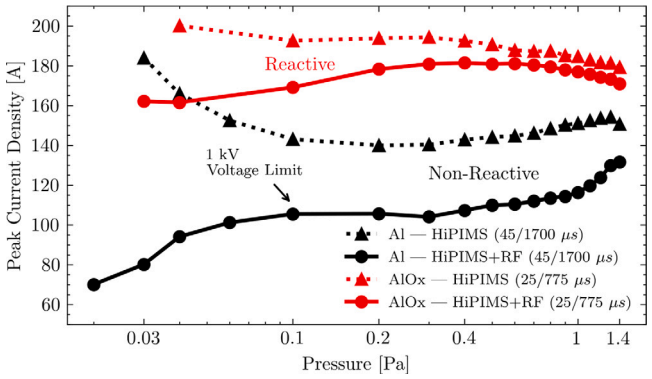

Fig. 9. Peak currents summarized from Figs. 5–8. Solid line represents non-reactive mode, dashed line represents reactive mode. The peak current densities in non-reactive mode are lower, compared to reactive mode. Furthermore, in the power controlled mode, the peak currents of the hybrid HiPIMS/RF are generally lower, compared to pure HiPIMS.

4. Discussion

Effect of RF superposition on peak current: In non-reactive mode, the superposition of RF power was expected to enhance pre-ionization, facilitate plasma ignition and thus increase the peak current of the subsequent HiPIMS pulse. Contrary to this expectation, we observed a suppression of the HiPIMS peak current when RF was superimposed, particularly at lower HiPIMS voltages. Such anti-assistance effects of an additional plasma on HiPIMS somewhat resembles earlier publications e.g. Anders et al. 2009 for a constricted MF plasma source [49]. While DC-excitation is mainly based on secondary electrons from the cathode surface, RF charge carriers are generated due to electron oscillations in the plasma bulk [40–42,50]. Taking also into account that the vicinity of the target surface is depleted of electrons [51], due to the RF-induced dark space, this might explain for the observed drop in HiPIMS current in superimposed HiPIMS+RF.

In the reactive case, the I–U characteristics for HiPIMS and superimposed HiPIMS+RF are very similar. Contrary to the non-reactive case, we have observed that the HiPIMS current in reactive deposition is increased, when RF power is added to the process.

The increased HiPIMS current in reactive HiPIMS+RF may be attributed to the significantly increased secondary electron emission coefficient (γ) for aluminium oxide (which has already formed on the target surface prior to the HiPIMS pulse) compared to pure aluminium ($\gamma = 1.2$ instead of $\gamma = 0.1$, see Corbella et al. [48]), leading to a high concentrations of electrons in the target vicinity and dominance of the HiPIMS discharge. This is somewhat similar to the observation of Bender et al. [41], where they superimposed RF and DC and observed a significant decrease in the discharge DC-voltage (power control mode) when only a small portion of RF-power was added.

Effect of pressure on peak current: The observed 'effect' of lower peak currents in reactive HiPIMS+RF mode, when compared to pure HiPIMS is not a physical but mainly technical effect due to the applied control mode as explained already in the results section and is again more prominent for the non-reactive case. When the current onset is delayed at lower pressures (Fig. 5), the time-integrated product of U*I over the pulse duration decreases and is counterbalanced by an increase of the voltage by the control software which, in turn, leads to very similar peak currents.

I-U Characterization: The different exponents n of the power law ($I = kU^n$) which were observed in the I-U characteristic for the non-reactive and reactive mode (Figs. 3 and 4) can be explained, according to Ehiasarian et al. [3] and Alami et al. [43] with different sputtering regimes. The exponent $n = 11$ for low current densities corresponds to DC-like sputtering, low plasma impedance and allows for a strong current increase at moderate voltage increase. One reason could be that some electrons can reach the cathode due to the superimposed RF voltage [52,53]. For current densities above approx. 500 mA/cm^2, the exponent n decreases to $n = 2.12$ which is attributed to a transition into HiPIMS-like plasma with high flux densities. In reactive mode, the plasma impedance is increased, resulting in generally lower values for n.

Self-Bias recovery dynamics: A notable observation is the difference in DC self-bias recovery dynamics between reactive and non-reactive modes. In the reactive process, the DC self-bias takes significantly longer (100 μs instead of 20 μs, compare figs. 8 and 6) to recover after the HiPIMS pulse at low pressures, which is the opposite of what is observed in non-reactive processes This behaviour is also tentatively ascribed to the higher density of secondary electrons in the reactive case which effectively shunts the dark space, thus delaying the formation of a potential drop above the target. First experiments with a ZrY-target indicate a similar behaviour for this different material and will be investigated in future works. Furthermore, the effect of an externally applied regular DC pre-ionization should be investigated in following works, in order to better understand the effects of RF induced DC self-bias.

In Summary, the findings suggests that the overall discharge dynamics are more complex than a simple additive effect, possibly involving a competition between the formation of a dark space and the inherent self bias in a RF-discharge, ionized particles and the generation of secondary electrons in the target vicinity as main charge carriers in pulsed processes like HiPIMS.

5. Conclusion

The present study provides new insights into the electrical behaviour and process stability of a hybrid HiPIMS+RF excitation scheme applied to a single magnetron assembly, for both non-reactive (Al) and reactive (AlO_x) sputtering processes. Our results demonstrate that superimposing RF power onto HiPIMS pulses alters the discharge characteristics, with significant implications for plasma ignition, peak current

behaviour, and operational pressure windows. While superimposing RF can increase the peak current in reactive HiPIMS+RF, the opposite was observed for the non-reactive process. The superimposed HiPIMS+RF process enables stable operation at lower pressures for both, non-reactive and reactive deposition, allowing stable plasma operation even at pressures as low as 0.03 Pa. This is particularly advantageous for the deposition of oxides and other compound materials, where low-pressure operation can improve film quality. At the same time, the suppression of peak current observed in non-reactive hybrid mode highlights the complex and sometimes counter-intuitive plasma interactions present in these systems. This complexity points to the need for further research, particularly in understanding the interplay of different plasma excitation mechanisms, charge carrier dynamics and resulting effects considering the properties of deposited thin films.

Future work will focus on plasma characterization, e.g. with time resolved ion energy and spectroscopic measurements, to elucidate the highly dynamical effects of the superimposed HiPIMS+RF mode and differentiate it from individual HiPIMS and RF discharges. Also, experiments with different target materials and different reactive gases (nitrogen instead of oxygen) are in preparation to further clarify the role of secondary electron emission yield and reactive gas ions. Simulations [54] of the investigated processes will also be performed and compared to experimental data.

CRediT authorship contribution statement

J. Müller: Writing – review & editing, Writing – original draft, Visualization, Project administration, Methodology, Investigation, Formal analysis, Conceptualization. **J. Swoboda:** Investigation, Conceptualization. **F. Burmeister:** Writing – review & editing, Supervision, Resources, Project administration, Methodology, Investigation, Conceptualization. **A. Fromm:** Writing – review & editing, Supervision, Methodology, Conceptualization. **M. Wirth:** Resources, Methodology. **A. Killinger:** Writing – review & editing. **S. Ulrich:** Writing – review & editing, Supervision.

Declaration of competing interest

The authors declare that they have no known competing financial interests or personal relationships that could have appeared to influence the work reported in this paper.

Acknowledgements

The project KK5079003KO2 “FastPIMS” was supported by the Federal Ministry of Economic Affairs and Energy as part of the ZIM program on basis of a decision by the German Bundestag. The authors wish to thank Aurion Anlagentechnik GmbH (Seligenstadt, Germany), PlasmaSolve (Brno, Czech Republic) and MELEC GmbH (Baden–Baden, Germany) for their valuable support and insightful discussions.

Data availability

Data will be made available on request.

References

[1] M. Ohring, Materials Science of Thin Films: Deposition and Structure, second ed., Academic Press, San Diego, California, 2002.

[2] V. Kouznetsov, K. Macák, J.M. Schneider, U. Helmersson, I. Petrov, A novel pulsed magnetron sputter technique utilizing very high target power densities, Surf. Coat. Technol. 122 (2–3) (1999) 290–293, http://dx.doi.org/10.1016/S0257-8972(99)00292-3.

[3] A. Ehiasarian, R. New, W.-D. Münz, L. Hultman, U. Helmersson, V. Kouznetsov, Influence of high power densities on the composition of pulsed magnetron plasmas, Vacuum 65 (2) (2002) 147–154, http://dx.doi.org/10.1016/s0042-207x(01)00475-4.

[4] K. Macák, V. Kouznetsov, J. Schneider, U. Helmersson, I. Petrov, Ionized sputter deposition using an extremely high plasma density pulsed magnetron discharge, J. Vac. Sci. Technol. A 18 (4) (2000) 1533–1537, http://dx.doi.org/10.1116/1.582380.

[5] J. Bohlmark, J. Alami, C. Christou, A.P. Ehiasarian, U. Helmersson, Ionization of sputtered metals in high power pulsed magnetron sputtering, J. Vac. Sci. Technol. A 23 (1) (2004) 18–22, http://dx.doi.org/10.1116/1.1818135.

[6] J. Alami, J.T. Gudmundsson, J. Bohlmark, J. Birch, U. Helmersson, Plasma dynamics in a highly ionized pulsed magnetron discharge, Plasma Sources Sci. Technol. 14 (3) (2005) 525–531, http://dx.doi.org/10.1088/0963-0252/14/3/015.

[7] J. Alami, S. Bolz, K. Sarakinos, High power pulsed magnetron sputtering: Fundamentals and applications, J. Alloys Compd. 483 (1–2) (2009) 530–534, http://dx.doi.org/10.1016/j.jallcom.2008.08.104.

[8] A. Anders, Discharge physics of high power impulse magnetron sputtering, Surf. Coat. Technol. 205 (2011) S1–S9, http://dx.doi.org/10.1016/j.surfcoat.2011.03.081.

[9] M. Samuelsson, D. Lundin, J. Jensen, M.A. Raadu, J.T. Gudmundsson, U. Helmersson, On the film density using high power impulse magnetron sputtering, Surf. Coat. Technol. 205 (2) (2010) 591–596, http://dx.doi.org/10.1016/j.surfcoat.2010.07.041.

[10] J. Alami, P.O.Å. Persson, D. Music, J.T. Gudmundsson, J. Bohlmark, U. Helmersson, Ion-assisted physical vapor deposition for enhanced film properties on nonflat surfaces, J. Vac. Sci. Technol. A: 23 (2) (2005) 278–280, http://dx.doi.org/10.1116/1.1861049.

[11] M. Lattemann, A. Ehiasarian, J. Bohlmark, P. Persson, U. Helmersson, Investigation of high power impulse magnetron sputtering pretreated interfaces for adhesion enhancement of hard coatings on steel, Surf. Coat. Technol. 200 (22–23) (2006) 6495–6499, http://dx.doi.org/10.1016/j.surfcoat.2005.11.082.

[12] A. Ehiasarian, J. Wen, I. Petrov, Interface microstructure engineering by high power impulse magnetron sputtering for the enhancement of adhesion, J. Appl. Phys. 101 (5) (2007) http://dx.doi.org/10.1063/1.2697052.

[13] A.P. Ehiasarian, High-power impulse magnetron sputtering and its applications, Pure Appl. Chem. 82 (6) (2010) 1247–1258, http://dx.doi.org/10.1351/pac-con-09-10-43.

[14] K. Bobzin, N. Bagcivan, P. Immich, S. Bolz, J. Alami, R. Cremer, Advantages of nanocomposite coatings deposited by high power pulse magnetron sputtering technology, J. Mater. Process. Technol. 209 (1) (2009) 165–170, http://dx.doi.org/10.1016/j.jmatprotec.2008.01.035.

[15] D.J. Christie, Target material pathways model for high power pulsed magnetron sputtering, J. Vac. Sci. Technol. A 23 (2) (2005) 330–335, http://dx.doi.org/10.1116/1.1865133.

[16] K. Sarakinos, J. Alami, M. Wuttig, Process characteristics and film properties upon growth of tioxfilms by high power pulsed magnetron sputtering, J. Phys. D: Appl. Phys. 40 (7) (2007) 2108–2114, http://dx.doi.org/10.1088/0022-3727/40/7/037.

[17] A. Anders, Deposition rates of high power impulse magnetron sputtering: Physics and economics, J. Vac. Sci. Technol. A 28 (4) (2010) 783–790, http://dx.doi.org/10.1116/1.3299267.

[18] P. Mareš, M. Dubau, J. Polášek, T. Mates, T. Kozák, J. Vyskočil, High deposition rate films prepared by reactive HiPIMS, Vacuum 191 (2021) 110329, http://dx.doi.org/10.1016/j.vacuum.2021.110329.

[19] M.P. Ferreira, D. Martínez-Martínez, J.-B. Chemin, P. Choquet, Tuning the characteristics of Al_2O_3 thin films using different pulse configurations: Mid-frequency, high-power impulse magnetron sputtering, and their combination, Surf. Coat. Technol. 466 (2023) 129648, http://dx.doi.org/10.1016/j.surfcoat.2023.129648.

[20] H. Larhlimi, M. Makha, J. Alami, Effect of pulse configuration on the reactive deposition of TiN coatings using HiPIMS, Surf. Coat. Technol. 473 (2023) 130024, http://dx.doi.org/10.1016/j.surfcoat.2023.130024.

[21] A. Anders, Physics of arcing, and implications to sputter deposition, Thin Solid Films 502 (1–2) (2006) 22–28, http://dx.doi.org/10.1016/j.tsf.2005.07.228.

[22] A. Anders, A review comparing cathodic arcs and high power impulse magnetron sputtering (hipims), Surf. Coat. Technol. 257 (2014) 308–325, http://dx.doi.org/10.1016/j.surfcoat.2014.08.043.

[23] V. Oskirko, V. Semenov, A. Solovyev, S. Rabotkin, A. Pavlov, A. Zakharov, Arc energy minimization in high-power impulse magnetron sputtering, Vacuum 202 (2022) 111213, http://dx.doi.org/10.1016/j.vacuum.2022.111213.

[24] A. Anders, Tutorial: Reactive high power impulse magnetron sputtering (R-HiPIMS), J. Appl. Phys. 121 (17) (2017) http://dx.doi.org/10.1063/1.4978350.

[25] D.J. Christie, W.D. Sproul, D.C. Carter, F. Tomasel, A novel pulsed supply with arc handling and leading edge control as enabling technology for high power pulsed magnetron sputtering (HPPMS), in: 47th Annual Technical Conference Proceedings, Society of Vacuum Coaters, 2004.

[26] V. Tiron, I.-L. Velicu, T. Matei, D. Cristea, L. Cunha, G. Stoian, Ultra-short pulse HiPIMS: A strategy to suppress arcing during reactive deposition of SiO_2 thin films with enhanced mechanical and optical properties, Coatings 10 (7) (2020) 633, http://dx.doi.org/10.3390/coatings10070633.

[27] N. Holtzer, O. Antonin, T. Minea, S. Marnieros, D. Bouchier, Improving HiPIMS deposition rates by hybrid RF/HiPIMS co-sputtering, and its relevance for NbSi films, Surf. Coat. Technol. 250 (2014) 32–36, http://dx.doi.org/10.1016/j.surfcoat.2014.02.007.

[28] B.-S. Lou, Y.-C. Yang, Y.-X. Qiu, W. Diyatmika, J.-W. Lee, Hybrid high power impulse and radio frequency magnetron sputtering system for ticrsin thin film depositions: Plasma characteristics and film properties, Surf. Coat. Technol. 350 (2018) 762–772, http://dx.doi.org/10.1016/j.surfcoat.2018.04.072.

[29] R. Bandorf, S. Falkenau, V. Schmidt, Modifications of coatings by DC-Sputtering with superimposed HPPMS, in: 50th Annual Technical Conference Proceedings, no. 0737-5921, Society of Vacuum Coaters, Society of Vacuum Coaters, 2007.

[30] R. Bandorf, S. Falkenau, K. Schiffmann, H. Gerdes, U. Heckmann, Properties of NiCr sputtered by HIPIMS in unipolar and DC-superimposed mode, in: 51st Annual Technical Conference Proceedings, no. 0737-5921, Society of Vacuum Coaters, Society of Vacuum Coaters, 2008.

[31] Q. Luo, S. Yang, K. Cooke, Hybrid HIPIMS and DC magnetron sputtering deposition of TiN coatings: Deposition rate, structure and tribological properties, Surf. Coat. Technol. 236 (2013) 13–21, http://dx.doi.org/10.1016/j.surfcoat.2013.07.003.

[32] M. Vergöhl, O. Werner, S. Bruns, T. Wallendorf, G. Mark, Superimposed MF-HiPIMS processes for the deposition of ZrO_2 thin films, in: 51th Annual Technical Conference Proceeding, Vol. 51, Society of Vacuum Coaters, 2008.

[33] G. Mark, E. Parra, R. Bandorf, M. Vergöhl, New superimposed pulsed plasma technology using high power impulse magnetron sputtering (HiPIMS) combined with DC or MF-frequency, in: 53rd Annual Technical Conference Proceedings, no. 0737-5921, 2010.

[34] F. Oelschlegel, Reaktive Abscheidung von Al_2O_3 durch Mittelfrequenz-überlagertes Hochleistungsimpuls-Magnetronsputtern (Ph.D. thesis), Technische Universität Dresden, 2012.

[35] W. Diyatmika, F.-K. Liang, B.-S. Lou, J.-H. Lu, D.-E. Sun, J.-W. Lee, Superimposed high power impulse and middle frequency magnetron sputtering: Role of pulse duration and average power of middle frequency, Surf. Coat. Technol. 352 (2018) 680–689, http://dx.doi.org/10.1016/j.surfcoat.2017.11.057.

[36] C.-Y. Lu, W. Diyatmika, B.-S. Lou, J.-W. Lee, Superimposition of high power impulse and middle frequency magnetron sputtering for fabrication of CrTiBN multicomponent hard coatings, Surf. Coat. Technol. 350 (2018) 962–970, http://dx.doi.org/10.1016/j.surfcoat.2018.03.045.

[37] C. Adam, Untersuchungen zur Plasmagestützten Abscheidung von Al_2O_3-Schichten im Reaktiven Hybriden und MF/HF-HiPIMS-Sputterprozess (Bachelor Thesis), University of Freiburg, 2023.

[38] J. Swoboda, Untersuchung Hybrider HF/HiPIMS-Prozesse und deren Wirkung auf die Materialeigenschaften und Defektdichte von SiAlOx-Schichten (Master's thesis), Stuttgart University, 2024.

[39] T. Tanaka, K. Kawabata, Preparation of ta/mo structure by using rf-dc coupled magnetron sputtering, Thin Solid Films 312 (1–2) (1998) 135–138, http://dx.doi.org/10.1016/s0040-6090(97)00727-x.

[40] K. Ellmer, R. Cebulla, R. Wendt, Characterization of a magnetron sputtering discharge with simultaneous RF- and DC-excitation of the plasma for the deposition of transparent and conductive ZnO:Al-films, Surf. Coat. Technol. 98 (1–3) (1998) 1251–1256, http://dx.doi.org/10.1016/s0257-8972(97)00253-3.

[41] M. Bender, J. Trube, J. Stollenwerk, Characterization of a RF/DC-magnetron discharge for the sputter deposition of transparent and highly conductive ITO films, 1999, http://dx.doi.org/10.1007/s003399900086.

[42] M. Stowell, J. Müller, M. Ruske, M. Lutz, T. Linz, RF-superimposed DC and pulsed DC sputtering for deposition of transparent conductive oxides, Thin Solid Films 515 (19) (2007) 7654–7657, http://dx.doi.org/10.1016/j.tsf.2006.11.166.

[43] J. Alami, K. Sarakinos, G. Mark, M. Wuttig, On the deposition rate in a high power pulsed magnetron sputtering discharge, Appl. Phys. Lett. 89 (15) (2006) http://dx.doi.org/10.1063/1.2362575.

[44] F. Magnus, O.B. Sveinsson, S. Olafsson, J.T. Gudmundsson, Current–voltage-time characteristics of the reactive ar/n2 high power impulse magnetron sputtering discharge, J. Appl. Phys. 110 (8) (2011) http://dx.doi.org/10.1063/1.3653233.

[45] J.T. Gudmundsson, Physics and technology of magnetron sputtering discharges, Plasma Sources Sci. Technol. 29 (11) (2020) 113001, http://dx.doi.org/10.1088/1361-6595/abb7bd.

[46] A. Anders, J. Andersson, A. Ehiasarian, High power impulse magnetron sputtering: Current–voltage-time characteristics indicate the onset of sustained self-sputtering, J. Appl. Phys. 102 (11) (2007) http://dx.doi.org/10.1063/1.2817812.

[47] D. Depla, S. Mahieu, R. De Gryse, Magnetron sputter deposition: Linking discharge voltage with target properties, Thin Solid Films 517 (9) (2009) 2825–2839, http://dx.doi.org/10.1016/j.tsf.2008.11.108.

[48] C. Corbella, A. Marcak, T. de los Arcos, A. von Keudell, Revising secondary electron yields of ion-sputtered metal oxides, J. Phys. D: Appl. Phys. 49 (16) (2016) 16LT01, http://dx.doi.org/10.1088/0022-3727/49/16/16lt01.

[49] A. Anders, G.Y. Yushkov, Plasma "anti-assistance" and "self-assistance" to high power impulse magnetron sputtering, J. Appl. Phys. 105 (7) (2009) http://dx.doi.org/10.1063/1.3097390.

[50] K. Ellmer, R. Cebulla, R. Wendt, Transparent and conducting ZnO(:Al) films deposited by simultaneous RF- and DC-excitation of a magnetron, Thin Solid Films 317 (1–2) (1998) 413–416, http://dx.doi.org/10.1016/s0040-6090(97)00633-0.

[51] J.T. Gudmundsson, D. Lundin, in: D. Lundin, T. Minea, J.T. Gudmundsson (Eds.), High Power Impulse Mangetron Sputtering: Fundamentals, Technologies, Challenges and Applications, Elsevier, Amsterdam, The Netherlands, 2020, pp. 1–48, Chap. 1.

[52] D. Depla, G. Buyle, J. Haemers, R. De Gryse, Discharge voltage measurements during magnetron sputtering, Surf. Coat. Technol. 200 (14–15) (2006) 4329–4338, http://dx.doi.org/10.1016/j.surfcoat.2005.02.166.

[53] B. Zheng, Y. Fu, K. Wang, T. Schuelke, Q.H. Fan, Electron dynamics in radio frequency magnetron sputtering argon discharges with a dielectric target, Plasma Sources Sci. Technol. 30 (3) (2021) 035019, http://dx.doi.org/10.1088/1361-6595/abe9f9.

[54] K. Tomanková, K. Mrózek, A. Obrusník, A. Fromm, F. Burmeister, Sensitivity analysis of various physics processes in industrial HiPIMS: A global plasma modelling perspective, Surf. Coat. Technol. 507 (2025) 132126, http://dx.doi.org/10.1016/j.surfcoat.2025.132126.